Published in "The Journal of Physical Chemistry B 120(29): 7244–7252, 2016"
which should be cited to refer to this work.

Universal Breakup of Colloidal Clusters in Simple Shear Flow

Yogesh M. Harshe[†] and Marco Lattuada[*,‡]

[†]Nestlé Research Center, Vers-chez-les-Blanc, CH-1000 Lausanne 26, Switzerland

[‡]Adolphe Merkle Institute, University of Fribourg, Chemin des Verdiers 4, CH-1700 Fribourg, Switzerland

ABSTRACT: We have studied the long-term dynamics of shear-induced breakage of individual colloidal clusters, covering a wide range of fractal dimensions, using Stokesian dynamics. We found that the time evolution of the normalized average size of the fragments generated by the breakup process could be scaled using a unique dimensionless time defined by multiplying the real time with the cluster breakage rate constant ($\tau = t \cdot k_B$). Clusters with different masses but the same fractal dimension exhibited almost identical breakage dynamics when exposed to equal overall hydrodynamic forces ($\eta\dot{\gamma}R_{g,0}^2$). The steady-state values of the average size, mass, and standard deviation of fragment mass distribution showed a universal scaling depending only on the overall hydrodynamic force, irrespective of the initial cluster properties. We also identified two asymptotic regimes for the evolution of the fractal dimension, $\langle d_f \rangle$, of fragments: open clusters ($d_f \leq 2.1$) produced dense fragments with a limiting $\langle d_f \rangle \approx 2.4 \pm 0.1$; conversely, dense clusters ($d_f \geq 2.5$) produced fragments with $\langle d_f \rangle \approx 2.5 \pm 0.1$.

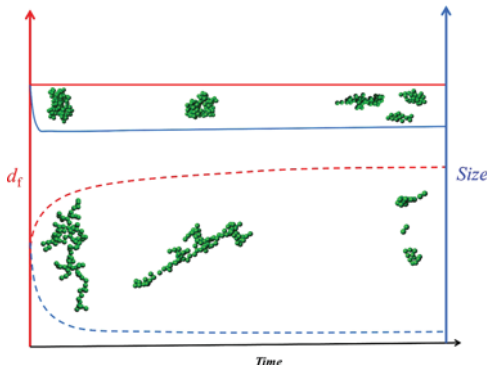

I. INTRODUCTION

Colloidal suspensions are one of the most commonly investigated model systems in soft-matter physics. They are also relevant in numerous processes of practical interest, such as in the production and/or processing of polymers and agricultural and food products, in wastewater treatment, and so forth. Whenever the colloidal stability of particles is compromised and attractive interactions dominate, particles tend to aggregate into clusters, which usually have a very irregular geometry and are described by means of fractal geometry concepts.[1−3] When colloidal aggregates are exposed to high shear rates, and therefore to strong hydrodynamic forces, their structure is deformed and collisions are enhanced, leading to both enhanced aggregation and breakage of clusters. Although shear-induced aggregation has been thoroughly studied in the literature through both experiments and simulations,[4−11] there is still a lack of understanding of cluster breakage, in spite of the experimental[12−23] and theoretical works[15,24−27] published. This is primarily due to the intricate entanglement of various physical phenomena occurring simultaneously.[20]

Quantifying the aggregate breakage process through experimental approaches has always been challenging because of the need for very fast and high-resolution measurement techniques to track the three-dimensional position of individual particles in the clusters.[28−30] For these reasons, scientists have used simulations to investigate the breakage of colloidal clusters. The most common techniques applied for this purpose are Langevin-type simulations, which follow the trajectory of individual particles in the clusters subject to known interactions. Typical interparticle interactions include standard colloidal interactions, such as attractive van der Waals forces and repulsive electrostatic or steric interactions, and in some instances, the discrete element method (DEM)[24,31,32] has been used to describe the contact forces of particles, the presence of which has been experimentally verified.[33] Where most of the simulation techniques differ substantially is in the description of hydrodynamic interactions among particles, which play a crucial role in properly describing the interactions of particles with the fluid. Several models have been used to account for hydrodynamic interactions, including lattice-Boltzmann simulation,[34] finite element method,[31] free-draining approximation,[35,36] and Stokesian dynamics (SD).[37−42] The free-draining approximation is the simplest and hence the most commonly used model in colloidal science because it completely neglects interparticle hydrodynamic interactions, thus substantially reducing the computational cost of the simulations. However, several publications have demonstrated the importance of including hydrodynamic interactions to properly describe the dynamics of hard spheres[43−45] and of interacting particles,[46,47] as well as the formation of colloidal gels.[48]

In recent publications,[49,50] we have investigated the breakage rate of colloidal clusters, covering a broad range of masses and fractal dimensions. To focus only on the breakage rate, we performed simulations only up to the very first binary breakage event experienced by a cluster. In this work, we have used the same modeling approach, based on SD, to investigate the breakup of colloidal aggregates under simple shear flow, when particles are subject to van der Waals attractive and Born short-

range repulsive interactions and contact forces described through DEM.[51] The objective here is to monitor the fate of an individual cluster for a sufficiently long time, until no further breakage events or structural modifications are observed in the overall population of produced fragments. A variety of new results have been obtained, which represent a substantial advancement in the field.

II. MODEL FORMULATION

The dynamic behavior of clusters is a complicated function of their structure and the fluid flow profile. The structure of a cluster is defined in terms of two quantities: coordination number and fractal dimension, representing respectively, the average number of nearest-neighbor particles of each particle in the cluster and the cluster density. These quantities affect both interparticle and hydrodynamic interactions. The first ones are short-ranged and are governed by the coordination number. The second ones, being much more long-ranged, are determined by the overall cluster morphology and structure and by its orientation relative to the flow. To properly describe a cluster behavior when exposed to shear forces, both interactions need to be accurately accounted for.

In this work, we have used the identical model methodology as described in our previous work,[49,50] which is briefly described in the following.

II.A. Hydrodynamic Contribution. For a multiparticle system, consisting of uniform-sized spherical particles in laminar flow, Stokes' law for a single particle has been successfully adapted by Brady and Bossis[39] into the so-called SD approach. In this method, the multipoles of forces acting on each particle in the system are related to the velocities of each particle. The force−torque−stresslet version of the SD model in the mobility form can be written as[52]

$$\begin{bmatrix} \bar{U}_n \\ \bar{\Omega}_n \end{bmatrix} = \begin{bmatrix} \bar{U}^{\infty} \\ \bar{\Omega}^{\infty} \end{bmatrix} + \begin{bmatrix} \bar{\bar{R}}_{FU} & \bar{\bar{R}}_{F\Omega} \\ \bar{\bar{R}}_{TU} & \bar{\bar{R}}_{T\Omega} \end{bmatrix}^{-1} \times \left[\begin{pmatrix} \bar{F}_n \\ \bar{T}_n \end{pmatrix} + \begin{pmatrix} \bar{\bar{\bar{R}}}_{FE} \\ \bar{\bar{\bar{R}}}_{TE} \end{pmatrix} : \bar{\bar{E}}^{\infty} \right] \tag{1}$$

Thus, the velocities (translational, $\bar{U}_n$, and angular, $\bar{\Omega}_n$) of each particle are linearly proportional to the forces ($\bar{F}_n$), torques ($\bar{T}_n$) acting on each particle, and the rate of strain ($\bar{\bar{E}}^{\infty}$), translational ($\bar{U}^{\infty}$), and angular velocities ($\bar{\Omega}^{\infty}$) of the applied flow evaluated at the center of the particle. The proportionality term is a complex tensorial quantity referred to as grand resistance matrix (R). The grand resistance matrix, R, can be represented in terms of submatrices as

$$R = \begin{bmatrix} R_{FU} & R_{F\Omega} & R_{FE} \\ R_{TU} & R_{T\Omega} & R_{TE} \\ R_{SU} & R_{S\Omega} & R_{SE} \end{bmatrix}_{11N\times 11N} = (M^{\infty})^{-1} + R_{2B}^{lub} - R_{2B}^{\infty} \tag{2}$$

the elements of which account for hydrodynamic interactions among particles and are functions of only the relative positions of the particles. The exact calculation of the grand resistance matrix cannot be carried out for more than two particles.[2,52−54] Therefore, a suitable approximation is necessary. In SD, the grand resistance is approximated by adding up different contributions: (1) inverse of the pair-wise additively found many-body far-field mobility (M^{∞}) and (2) exact two-body lubrication resistance (R_{2B}^{lub}), from which the exact two-body far-field resistance interaction matrix (R_{2B}^{∞}) is subtracted to avoid double counting of the two-body far-field interactions.

In the present work, we have adopted this procedure as the method has been proven to work at very large solid volume fractions; hence, it accounts for multibody hydrodynamic interactions accurately and can be virtually extended to any number of particles.[39,52]

II.B. Interparticle Interactions. In a suspension, the hydrodynamic force acting on one particle is transmitted to the other particles either through the particle−fluid−particle, also called hydrodynamic interactions, or via other particle−particle interactions. The propagation mechanism with interparticle interactions encompasses two classes of phenomena, namely, contact and noncontact interactions, with the former acting only when two particles are touching each other.[55] These are briefly described in the following.

II.B.1. Noncontact Interactions. The most common type of colloidal interactions that particles experience are attractive and repulsive interactions, commonly described by Derjaguin−Landau−Verwey−Overbeek theory.[56,57] The theory accounts for the London−van der Waals attractive and electrostatic repulsion potentials between charged nontouching surfaces of particles, and the net potential energy is the sum of these two. In the present work, we have considered only van der Waals interactions, which occur when electrostatically stabilized particles are under fully destabilized conditions. The van der Waals attractive potential is given by the Hamaker equation

$$V_{vdw}(s) = -\frac{A_h}{6}\left[\frac{2}{s^2-4} + \frac{2}{s^2} + \ln\left(\frac{s^2-4}{s^2}\right)\right] \tag{3}$$

where A_h is the nonretarded Hamaker constant and s is the dimensionless distance between the pair of particles, $s = r/R_p$, where r is the actual distance between the centers of particles and R_p is the primary particle radius.

In addition, to prevent particles from overlapping, a short-range Born repulsive potential has been introduced, which is given by

$$V_{born}(s) = \frac{A_h N_{born}}{s}\left[\frac{s^2-14s+54}{(s-2)^7} + \frac{60-2s^2}{s^7} + \frac{s^2+14s+54}{(s+2)^7}\right] \tag{4}$$

where N_{born} is the Born repulsion constant.

It must be noted here that, as opposed to some other research works[42,58] dealing with the breakup of colloidal aggregates and taking into account colloidal particle−particle interactions, no arbitrary bounds have been imposed on the potentials.

II.B.2. Contact Interactions. Recently, Pantina and Furst[59−61] have experimentally demonstrated that tangential contact interactions among particles are responsible for providing bending strength to interparticle bonds and should be incorporated to correctly describe the dynamics of chains of particles. These interactions have been already included in computer simulations by Becker and Brisen[62] using a DEM approach.[51] In the present work, we have adopted their approach to estimate the relative tangential velocities and hence the relative tangential force, which are present when two particles are separated by a very small distance (δ_{min} = 3 Å for particles with a radius of 1 μm), corresponding to the minimum

of the potential interaction curve. For colloidal particles to be considered, connected values of interparticle distance equal to several angstroms are reported in the literature.[57,63] The force (F^t) and torque (T^t) due to the tangential interactions are estimated as follows

$$\overline{F}_j^t = K_t(\overline{\xi}_{ij} - \overline{\xi}_{ji})$$
$$\overline{T}_j^t = 2R_pK_t\overline{n}_{ij} \times \overline{\xi}_{ij} \quad (5)$$

where K_t is the coefficient of tangential rigidity, $\overline{\xi}$ is the length of the tangential displacement of the spring between the connected particles, and $\overline{n}$ is the normal vector connecting the centers of two particles, i and j. The tangential spring is broken when its length exceeds the maximum value of the relative tangential displacement, $\overline{\xi}_{max}$, which is obtained as described by Becker and Briesen[62] and using the same set of parameters as reported in their paper.

III. SIMULATION METHODOLOGY

We used an in-house cluster library, generated using various Monte Carlo algorithms, containing clusters with a wide range of morphologies (i.e., fractal dimensions) and masses. All our clusters follow the fractal scaling law

$$N = k_f\left(\frac{R_g}{R_p}\right)^{d_f} \quad (6)$$

where N is the number of primary particles in the cluster, R_p is the primary particle size, R_g is the radius of gyration of the cluster, k_f is a prefactor, which has usually a value close to 1, and d_f is the fractal dimension of the cluster. Here, N also represents the mass of the cluster as all particles are uniform-sized spheres made of the same material. The structures of typical initial clusters with different fractal dimensions (morphologies) are shown in Figure 1a. It is of paramount importance to note that a true fractal object should exhibit self-similarity. This is clearly not the case here, considering that the clusters used in this work are rather small. Under these circumstances, the exponent d_f in eq 1 should be considered as a mass−size scaling exponent more than a real fractal dimension. Nevertheless, it is rather common in the literature to refer to this exponent as fractal dimension; hence, we maintain this denomination throughout this work.

The range of applied shear stresses ($\sigma = \eta_f\gamma$, where η_f is the fluid viscosity and γ is the shear rate) between 25 and 100 Pa was found to be suitable to study the complete breakup dynamics of our aggregates in a reasonable computational time. These applied stresses correspond to Péclet numbers, $\mathrm{Pe} = \frac{R_g^2\gamma}{D} = \frac{6\eta_f\gamma R_g^3}{k_BT}$, where D is the diffusion coefficient, k_B is the Boltzmann constant, and T is the ambient temperature, for particles in water in the order of 10^5, which also justifies our choice of neglecting the Brownian motion of individual particles. A schematic of the initial position of the cluster in the flow field is shown in Figure 1b. The origin of the Cartesian axes was chosen at the center of mass of the original cluster.

A cluster of given mass and fractal dimension was randomly chosen from our cluster library. The clusters used in the present work are randomly chosen from an in-house cluster library. Various Monte Carlo algorithms were used to generate clusters with different properties (d_f, N). However, the generated clusters were not energetically stable in the configuration at the beginning of the simulation as the particles were arranged by random contact while generating the clusters. Hence, the clusters were not in the minimum-energy configurations. The distances between particles at contact, for the clusters produced with Monte Carlo simulations, are defined within a small tolerance but without accounting for any interparticle interactions. A small initial overlap among particles in contact due to tolerance has a strong effect on interparticle interactions. This required equilibration of the clusters, wherein the particles were allowed to move with respect to each other, however in the absence of fluid flow, for the clusters to attain an energetically stable structure. It must be noted that, as a result of equilibration, only minimal particle displacements were observed, without any effect on the overall structure (radius of gyration or fractal dimension) of the original cluster.

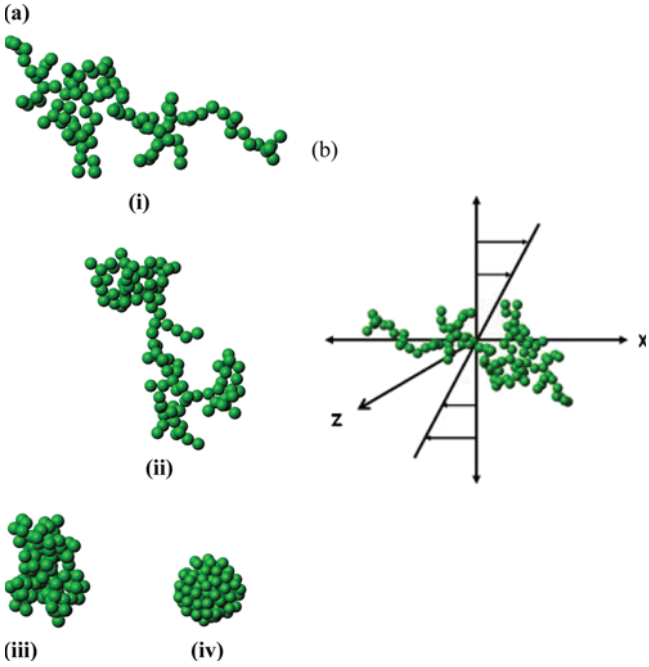

Figure 1. (a) Representative colloidal clusters used in the present work, d_f = (i) 1.8, (ii) 2.1, (iii) 2.5, and (iv) 3.0. (b) Schematic of a typical simple shear flow field to which a cluster is exposed to.

After equilibration, the actual simulation was started, wherein by knowing the relative positions of all particles, the hydrodynamic resistance matrix and the interparticle interactions were computed. Once all interparticle forces and fluid velocities at the center of each particle are known, their velocities, and hence the displacements of individual particles, were computed using the SD model. The critical distance, s_{break}, below which two particles were still considered connected, has been set to 2 nm. This is also where the value of total potential dropped to 1/4th and the attractive force to 2% of its value at the minimum of the potential well. At each time step, the number of fragments produced and the size of each fragment were calculated. All simulations were performed until a steady state was reached by monitoring the evolution of the average radius of gyration $\langle R_g \rangle$ of the fragment normalized by the radius of the particle. The time required to attain a steady state is large and increases with the cluster mass. Hence, we have performed most simulations for the specific case of clusters with a mass N = 60. The number of clusters that could be simulated in a reasonable time was restricted by two important factors. First of all, as the number of particles in a cluster increases, the

computational efforts required for estimating the hydrodynamic resistance matrix increase substantially (being proportional to $\sim(11N)^3$ times) as inverting the far-field mobility matrix is the bottleneck of the whole simulation method. Second, very small time steps, $\Delta t = 10^{-10}-10^{-9}$ s, are required to avoid overlapping of particles.

To understand the role of initial cluster morphology, a range of cluster morphologies ($d_f = 1.8-3.0$) were considered, covering practically occurring three classes of colloidal aggregates: open clusters ($d_f = 1.8, 2.1$), moderately dense clusters ($d_f = 2.5$), and very dense clusters ($d_f = 3.0$). For each cluster fractal dimension, 10 different cluster realizations were simulated to obtain statistically representative results.

IV. RESULTS AND DISCUSSION

We have studied the dynamics of evolution of fragments produced by the breakup of aggregates, focusing primarily on the clusters composed of 60 particles with primary particle radius of 1 μm, covering a broad range of fractal dimensions ($d_f = 1.8-3.0$) and applied shear stresses ($\sigma = \eta_f\gamma = 25-100$ Pa).

At first, we have looked at the time evolution of the average size and size distribution and the fractal dimension of the fragments produced. In all cases, we introduced a dimensionless time, τ, defined as the product of the physical time (t) and the cluster breakage rate constant (k_B) derived from our previous work,[49] that is, $\tau = k_B t$. Considering the size evolution of the fragments, we have defined the following dimensionless size: $\langle R_g' \rangle = \left(\frac{\langle R_g \rangle - \langle R_{g,s} \rangle}{R_{g,0} - \langle R_{g,s} \rangle} \right)$, where $\langle R_g \rangle$ and $\langle R_{g,s} \rangle$ are the weight-average radii of gyration of the entire fragment population at any time t and at a steady state, respectively. As $R_{g,0}$ is the dimensionless radius of gyration of the original cluster (i.e., normalized by the primary particle radius), the value of $\langle R_g' \rangle$ ranges from 1 at the beginning to 0 at the steady state. The time evolution of $\langle R_g' \rangle$ against τ is shown in Figure 2a,b for clusters with $d_f = 1.8$ and 2.5, respectively, for various applied stresses σ along with the representative snapshots of the initial cluster and the evolution of the fragments produced.

It can be observed that $\langle R_g' \rangle$ decreases exponentially, following a trend almost independent of the applied shear stress value but only depending on the cluster fractal dimension, even though the dimensional $\langle R_g \rangle$ values at a given time and for different applied stresses σ are different. This indicates that the breakage rate, obtained from very short simulation times, defines the appropriate characteristic time even for the long-term breakage process. We have fitted an exponential decaying function to model the decrease in dimensionless size with time. The exponential factor α is a function of only the fractal dimension, and for $d_f = 1.8$, 2.1, 2.5, and 3.0, we found $\alpha = 0.07$, 0.05, 0.02, and 0.015, respectively. The values of α indicate that the decay dynamics of clusters becomes slower as the fractal dimension increases.

The simulations indicate that open clusters show a rapid reduction in the average cluster size, whereas dense clusters show a sluggish decrease of the average fragment size along with an oscillatory behavior, with values of $\langle R_g' \rangle$ reaching larger than 1 immediately after imposing the shear. This behavior is particularly prominent at low shear rates. This means that open clusters are prevalently broken by the application of shear, whereas denser clusters show breakage accompanied by cluster deformation and restructuring, with a more pronounced effect at low shear stresses. The dynamics for two extremes of the

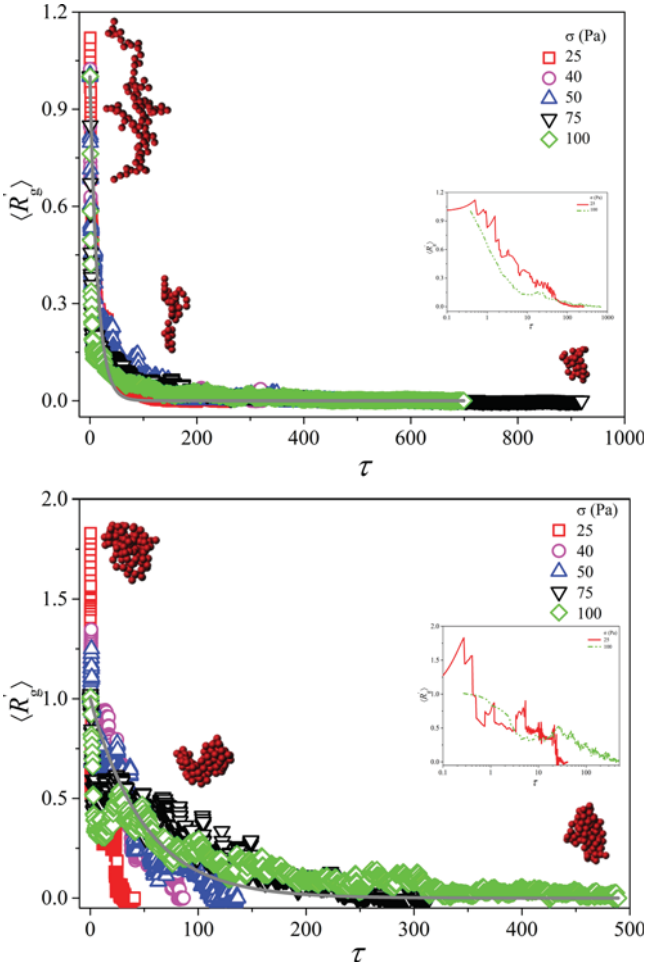

Figure 2. Evolution of $\langle R_g' \rangle$ as a function of τ for $N = 60$ for clusters with two different fractal dimensions: $d_f = 1.8$ (a) and 2.5 (b). The fitted trend line is obtained with $\langle R_g' \rangle \sim \exp(-\alpha\tau)$.

applied stresses for two different cluster morphologies is shown in the insets in Figure 2a,b. This is consistent with the observation that high shear rates promote breakage whereas lower shear rates promote restructuring of clusters. The results also indicate that a dense cluster is more resistant to any applied shear rate than an open cluster. Furthermore, it can be seen that this conclusion is very well supported by the included snapshots of the fragments produced along the evolution of $\langle R_g' \rangle$. The dimensionless time required for reaching the steady state increases with increasing fractal dimension. For open clusters, the steady state is reached monotonically at $\tau \sim 50$ for all applied stress values, whereas for initially dense clusters, larger values of $\tau \sim 100-150$ are required.

In the case of dense clusters, at intermediate times, the scaled size shows oscillations, which reflect a combination of restructuring of the fragments, indicating successive stretching and compression phases imposed by simple shear conditions. Compared to an open cluster, a dense cluster is smaller in size and thus experiences a smaller overall hydrodynamic force for the same shear rate. Moreover, in a dense cluster, there is also a screening effect of hydrodynamic stress due to a more compact structure. Under these conditions, a dense cluster is more prone to restructuring than an open one. Figure 2b also shows that $\langle R_g' \rangle$ rapidly increases first, then decays, and then undergoes oscillations, which are highly cluster specific. It is clear that the simple exponential decay is not able to account completely for

such a trend. This also means that not only the first event of breakage but also the overall breakup dynamics of denser clusters is slower than that of the open clusters.

As colloidal dispersions typically also consist of aggregates covering a broad range of masses, we investigated the dynamics of clusters with different initial number of particles. A simple scaling argument to estimate the total hydrodynamic force experienced by a cluster subject to a simple shear flow leads to the following result; that is, $F_{\text{hydro}}^{\text{cluster}} \sim \sigma R_{g,0}^2$, which means that the hydrodynamic force is proportional to the square of the cluster size and the applied stress. We decided to see whether the clusters with the same fractal dimension but different number of particles (N = 60 and 100) would show the same long-term breakage dynamics when subject to the same hydrodynamic force. The evolution of $\langle R_g' \rangle$ for a few clusters satisfying this requirement is presented in Figure 3a,b for two

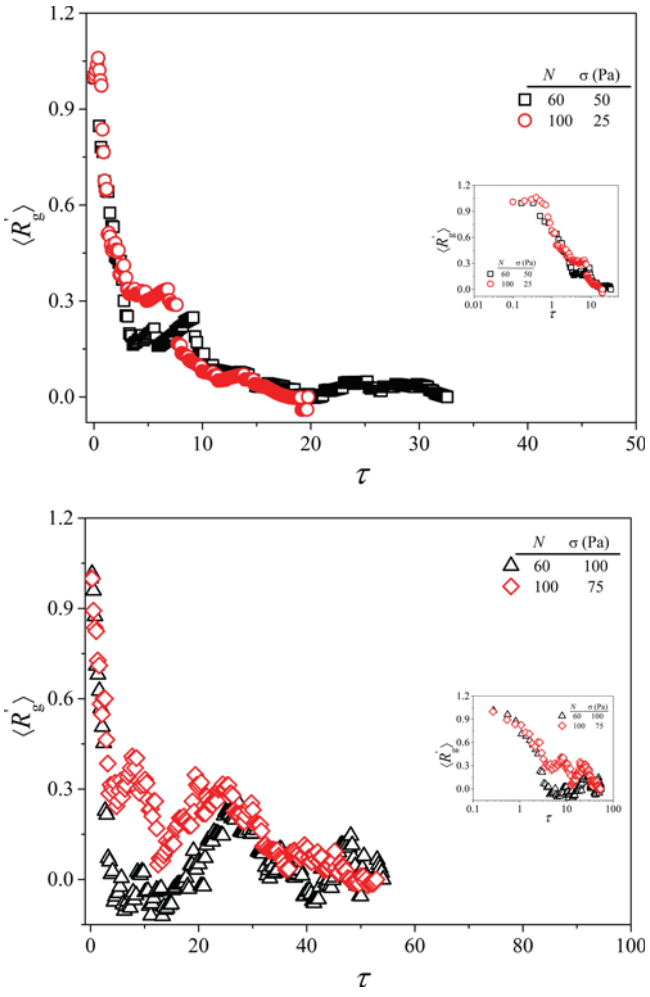

Figure 3. Dynamics of breakup for clusters with different cluster masses but with the same total hydrodynamic force applied for two different fractal dimensions: (a) 1.8 and (b) 2.5.

different cluster fractal dimensions (d_f = 1.8 and 2.5). A semilog plot as an inset in the figures shows this behavior clearly. From the figure, it can be seen that the evolution of $\langle R_g' \rangle$ is almost independent of the initial number of particles in the cluster and the applied stress, as long as the total hydrodynamic force applied on the clusters is kept constant when plotted as a function of the dimensionless time τ. These results indicate that the total hydrodynamic force acting on the clusters of a specific fractal dimension and their short-term breakage rate are the dominant factors for their long-term breakage dynamics. This motivated us to concentrate our computational efforts in investigating the dynamic behavior of the clusters of a fixed number of particles. Therefore, unless explicitly stated, all of the results discussed here have been obtained from the simulations of clusters having N = 60.

In addition to the cluster size, the simulations allowed us to monitor also the evolving fragment morphology in terms of their fractal dimension. Very few attempts have been reported in the literature[20,26,64] to keep track of the fractal dimension during the breakup process of an aggregate. Here, we have studied the evolution of the fractal dimension of the fragments under various conditions. The fractal dimensions have been obtained from a power law fit of the masses versus sizes of the fragments produced by the breakup of a few clusters with the same cluster mass and fractal dimension, excluding single particles and doublets. In Figure 4, the evolution of the fractal

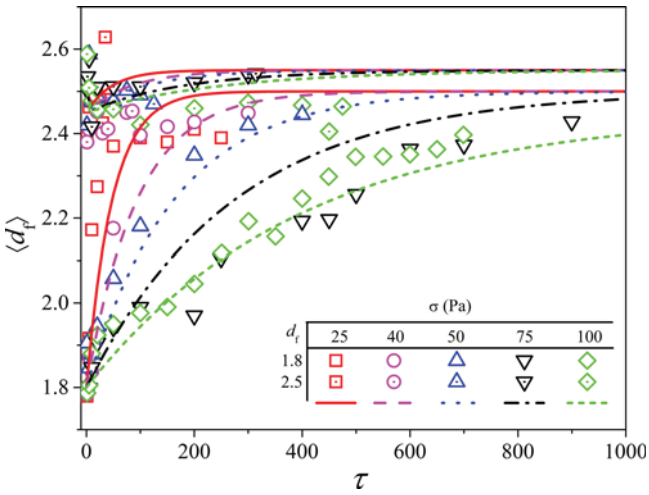

Figure 4. Evolution of average fractal dimension $\langle d_f \rangle$ for the breakup of clusters with N = 60. The lines are fitted using $\langle d_f \rangle = d_f + (\langle d_{f,ss} \rangle - d_f)\left(1 - \exp\left(-\frac{\tau}{\sigma^{1.3}}\right)\right)$, with $\langle d_{f,ss} \rangle$ = 2.4 for d_f = 1.8 and $\langle d_{f,ss} \rangle$ = 2.6 for d_f = 2.5.

dimension of fragments starting with open (d_f = 1.8) and moderately dense (d_f = 2.5) clusters under different shear stresses has been presented. It can be seen from the figure that initially open clusters tend to produce denser fragments and increase their fractal dimension to a limiting value. The increase in the fractal dimension can be explained as a result of the breakup of clusters combined with their densification, as a consequence of the exposure to compressive and extensional stresses during cluster rotation, in accordance with what was reported by Harshe et al.,[20] Tang et al.,[64] Harada et al.,[42] and Seto et al.[65] In all of these works, the authors observed densification of initially open clusters as an effect of flow with a rotational component. One should also notice that no universal master curve has been obtained in this case because the growth of the fractal dimension can be well fitted with an exponential curve, with a characteristic time depending on the shear rate. Such an empirical function has already been used in the literature by Harada et al.[58] Furthermore, though not shown in the figure, we observed similar behavior for clusters with initial d_f = 2.1. On the other hand, it is interesting to note that moderately dense clusters with d_f = 2.5 do not change their

structure much, as indicated by the fractal dimension of the fragments produced, which remains around 2.6 during the entire breakup process, independent of the applied stress. This is in agreement with the experimental results of Soos et al.[16] for the breakup of already dense clusters with d_f = 2.7, in which they found that the clusters after breaking into smaller fragments did not change the morphology and the aspect ratio. For initially very dense clusters (d_f = 3.0), also not shown in the figure, we noticed that first there is a sharp reduction in their fractal dimension to a value around 2.6, which then remained almost constant over time for all applied stresses. This is typically the value experimentally measured under shear-induced aggregation.[16] In our case, we have considered only single aggregates so that no reaggregation is present, as the simulations are carried out under infinite dilution. From this discussion, it can be inferred that there are two regimes for the evolution of fractal dimension. The first one is the regime for which the upper limiting value of $\langle d_f \rangle \leq 2.5$, where clusters with low fractal dimension (or open structures) are densified, producing denser fragments, and the steady state d_f value is governed by the applied stress and by the original d_f values. The second region is where $\langle d_f \rangle \approx 2.6$, in which the clusters with initial $\langle d_f \rangle \geq 2.6$ keep the fractal dimension almost unchanged, whereas very dense clusters (d_f = 3.0) decrease their d_f, reaching lower limiting fractal dimension values around 2.6. These two regimes can be clearly seen in Figure 4.

This densification of clusters along the breakup process was also confirmed when the dynamics of the coordination number ($\langle C_o \rangle$), defined as the average number of nearest neighbors per particle, was followed. This evolution in terms of approaching steady-state coordination number ($\langle C_o^s \rangle - \langle C_o \rangle$) for different applied stresses is shown in Figure 5a,b for clusters with d_f = 1.8 and 2.5, respectively. From the figures, it can be seen that the dynamics of ($\langle C_o^s \rangle - \langle C_o \rangle$) collapses on a single curve irrespective of the applied stress and an exponential function similar to the one suggested by Harada et al.[58] can be used to capture the trend. We fitted the data using $\langle C_o^s \rangle - \langle C_o \rangle = \lambda \exp(\varphi\tau)$, shown by a solid line, and found values of φ = −0.015 and −0.05 for d_f = 1.8 and 2.5, respectively, and λ = 2.75, indicating that the dynamics required to reach the steady-state compaction is faster for a denser aggregate. The reason behind this behavior lies in the shorter path that particles need to cover to increase the number of their bonds. The figures also indicate that the internal structure of aggregates is modified and the produced fragments have a higher average number of bonds, as a result of breakage and restructuring. This is not surprising, given that Monte Carlo-generated clusters have statistically only two bonds per particle. The coordination number increases exponentially, as reported in the literature,[40] but reached lower values for higher shear rates, when breakage dominates.

We have eventually focused our attention to the steady-state properties of clusters, using the total hydrodynamic force initially acting on the cluster, $\sigma R_{g,0}^2$, as a scaling quantity. We have plotted against $\sigma R_{g,0}^2$ in Figure 6a–c three important properties of the fragments: their average size normalized by the initial cluster size, their average mass normalized by the initial cluster mass, and the standard deviation of their mass distribution, respectively. On a double-log plot, all of these properties showed a linear dependence on $\sigma R_{g,0}^2$, irrespective of the initial cluster size, mass, and fractal dimension. This implies that data for all cluster masses collapse on a single master curve, which can be used to determine the steady-state values of these parameters, knowing the applied stress and the initial cluster

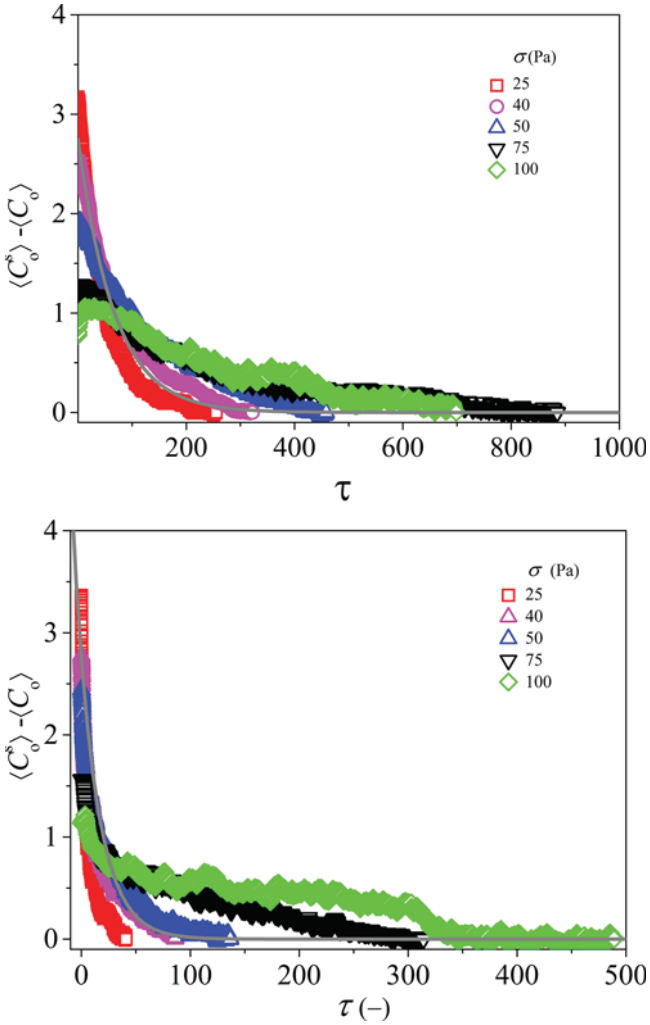

Figure 5. Evolution of average coordination number, $\langle C_o \rangle$, of fragments for clusters with N = 60 and d_f = 1.8 (a) and 2.5 (b) for different applied shear stresses, and the solid line is fitted with $\langle C_o^s \rangle - \langle C_o \rangle = \lambda \exp(\varphi\tau)$: φ = −0.015 and −0.05 for d_f = 1.8 and 2.5, respectively, and λ = 2.75.

properties. This data set can be combined with the scaled $\langle R_g' \rangle$ dynamics from Figure 2 to determine the complete breakup dynamics of a cluster in terms of actual evolution of the average fragment size, $\langle R_g \rangle$. Moreover, it should be noted that for very small values of the overall hydrodynamic force, the normalized fragment size and mass reach a plateau value very close to 1, indicating the critical force that the cluster can survive without breakage. In Figure 6a, we have also included the experimental data points from the work of Soos et al.[16] and Harshe et al.[20] to compare with our proposed scaling law. In both works, researchers have followed breakup of clusters with two different fractal dimensions (d_f = 1.7 and 2.7) composed of primary particles of two different sizes (R_p = 45 and 405 nm) in a contracting nozzle until a steady state was reached. Here, knowing the steady-state average fragment size for a specific applied stress, starting with a particular size of the initial aggregate, we have produced the data points. It can be seen that the proposed scaling very well compares with the already established experimental data. This comparison strengthens the finding of our scaling laws for universal behavior of colloidal aggregates when exposed to flow. A single fracture exponent for all quantities as a function of the total hydrodynamic force,

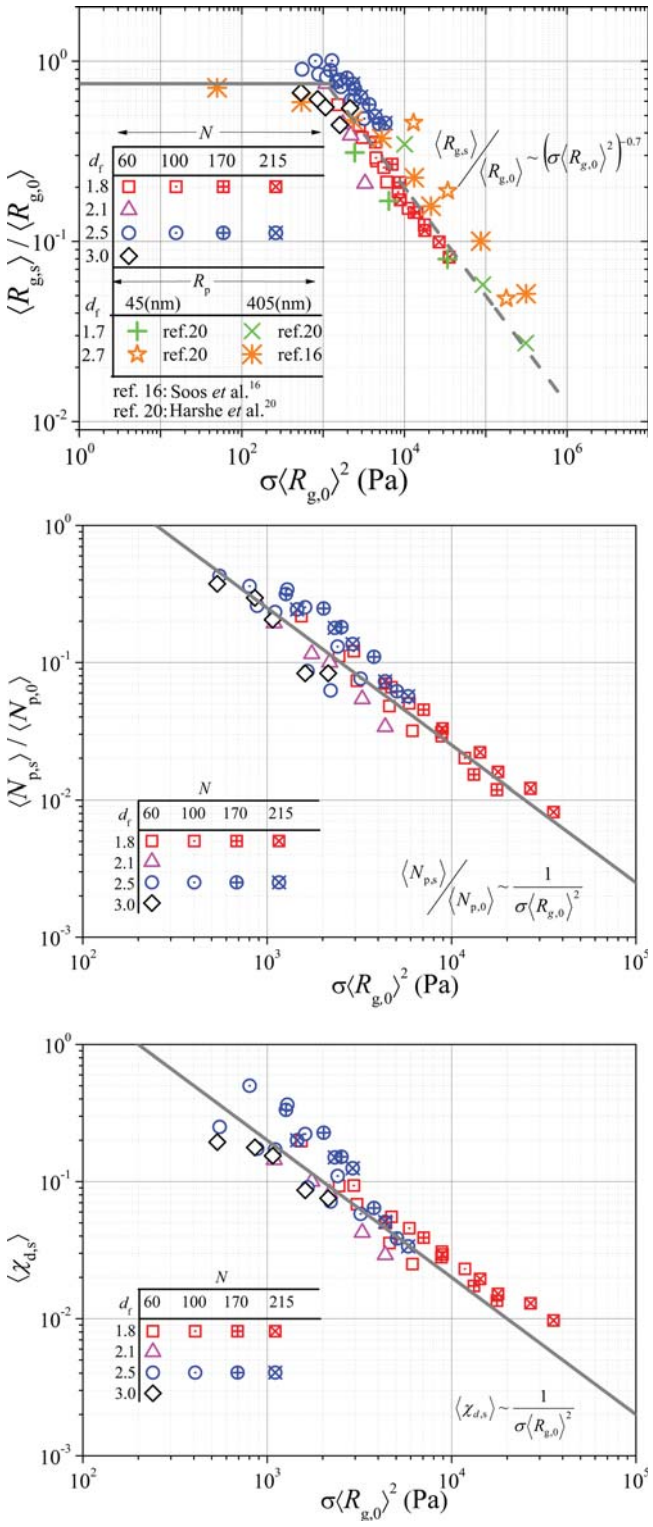

Figure 6. Steady-state average radius of gyration $\langle R_{g,s}\rangle$ (a) and number of particles $\langle N_{p,s}\rangle$ (b), respectively, normalized by initial cluster size $R_{g,0}$ and number of particles $N_{p,0}$ in the original cluster, and standard deviation $\langle \chi_{d,s}\rangle$ (c) of fragment mass distribution against the total hydrodynamic force $\sigma R_{g,0}^2$ on the original cluster.

$\sigma R_{g,0}^2$, acting on the cluster, independent of the initial cluster fractal dimension, can be explained by observing that the structure of all clusters exposed to high shear rates tends to evolve toward similar values of fractal dimension, independent of their initial structure. This observation is further supported by the data presented in Figure 7, where the steady-state fragment size is plotted against the fragment mass for different

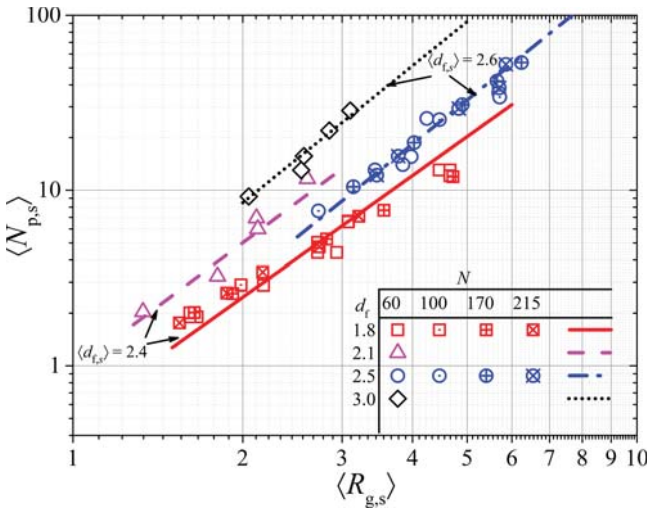

Figure 7. Steady-state average number of particles in fragment $\langle N_{p,s}\rangle$ vs average fragment size $\langle R_{g,s}\rangle$, for breakup of clusters with different initial fractal dimensions. Lines are fitted to simulation data with the slopes indicated by $\langle d_{f,s}\rangle$.

initial cluster fractal dimensions. The fitted lines for each of the data set showed a scaling representing the average fragment fractal dimension. This also confirms our finding from Figure 4 that there exist two regimes of fragment morphologies depending on the initial cluster morphology.

V. CONCLUSIONS

In conclusion, we have studied the long-term breakup dynamics of colloidal aggregates made of monodisperse spherical particles using SD. We found that the specific time evolution of the normalized cluster size shows a master curve dependence and is governed by only the initial cluster, d_f. The dynamics of evolution can also be scaled appropriately for clusters of different masses but the same fractal dimension if the overall hydrodynamic force is kept constant. Moreover, the steady-state average fragment size, mass, and mass distribution were found to be uniquely related to this overall hydrodynamic force acting on a cluster, irrespective of the mass and morphology of the initial cluster. The proposed scaling law for the dependence of the normalized average radius of gyration of fragments against the overall hydrodynamic force acting on the original cluster is in very good agreement with the already published experimental data by Soos et al.[16] and Harshe et al.[20] Thus, the suggested scaling laws can be used to determine the steady-state properties of the produced fragments after a breakup process. Finally, the dynamics of fragment fractal dimension showed two distinctive regimes, depending on the initial cluster morphology: initially open clusters produced denser fragments with asymptotic $\langle d_f\rangle \approx 2.4$, and dense clusters lead to fragments with $\langle d_f\rangle \approx 2.6$. These results are in agreement with the limited data available in the literature and further enhance the scope of such observations. All of these results contribute to rationalize the phenomena involved during the breakup process of a colloidal aggregate under simple shear and could be further validated by performing controlled experiments.

AUTHOR INFORMATION

Corresponding Author

*E-mail: marco.lattuada@unifr.ch.

Notes

The authors declare no competing financial interest.

ACKNOWLEDGMENTS

The authors are thankful to Prof. Dr. Massimo Morbidelli for his valuable suggestions to the work. The work was financially supported by the Swiss National Foundation (Grant Nos. 200020_126487/1 and PP00P2133597/1).

REFERENCES

(1) Brenner, H.; Condiff, D. W. Transport Mechanics in Systems of Orientable Particles. 3. Arbitrary Particles. *J. Colloid Interface Sci.* **1972**, *41*, 228−274.

(2) Kim, S.; Karrila, S. J. *Microhydrodynamics: Principles and Selected Applications*; Butterworth-Heinemann: Boston, 1991; p xxiii.

(3) Moncho-Jorda, A.; Louis, A. A.; Padding, J. T. Effects of Interparticle Attractions on Colloidal Sedimentation. *Phys. Rev. Lett.* **2010**, *104*, No. 068301, DOI: 10.1103/PhysRevLett.104.068301.

(4) Ehrl, L.; Soos, M.; Morbidelli, M.; Babler, M. U. Dependence of Initial Cluster Aggregation Kinetics on Shear Rate for Particles of Different Sizes under Turbulence. *AIChE J.* **2009**, *55*, 3076−3087.

(5) Kusters, K. A.; Wijers, J. G.; Thoenes, D. Aggregation Kinetics of Small Particles in Agitated Vessels. *Chem. Eng. Sci.* **1997**, *52*, 107−121.

(6) Babler, M. U. A Collision Efficiency Model for Flow-Induced Coagulation of Fractal Aggregates. *AIChE J.* **2008**, *54*, 1748−1760.

(7) Babler, M. U.; Moussa, A. S.; Soos, M.; Morbidelli, M. Structure and Kinetics of Shear Aggregation in Turbulent Flows. I. Early Stage of Aggregation. *Langmuir* **2010**, *26*, 13142−13152.

(8) Soos, M.; Sefcik, J.; Morbidelli, M. Master Curves for Aggregation and Gelation: Effects of Cluster Structure and Polydispersity. *Ind. Eng. Chem. Res.* **2007**, *46*, 1709−1720.

(9) Potanln, A. A. On the Microrheological Modeling of Aggregating Colloids. *J. Dispersion Sci. Technol.* **1992**, *13*, 527−548.

(10) Potanin, A. A. On the Model of Colloid Aggregates and Aggregating Colloids. *J. Chem. Phys.* **1992**, *96*, 9191−9200.

(11) Oles, V. Shear-Induced Aggregation and Breakup of Polystyrene Latex-Particles. *J. Colloid Interface Sci.* **1992**, *154*, 351−358.

(12) Sonntag, R. C.; Russel, W. B. Structure and Breakup of Flocs Subjected to Fluid Stresses. 1. Shear Experiments. *J. Colloid Interface Sci.* **1986**, *113*, 399−413.

(13) Sonntag, R. C.; Russel, W. B. Structure and Breakup of Flocs Subjected to Fluid Stresses. 2. Theory. *J. Colloid Interface Sci.* **1987**, *115*, 378−389.

(14) Sonntag, R. C.; Russel, W. B. Structure and Breakup of Flocs Subjected to Fluid Stresses. 3. Converging Flow. *J. Colloid Interface Sci.* **1987**, *115*, 390−395.

(15) Higashitani, K.; Inada, N.; Ochi, T. Floc Breakup Along Centerline of Contractile Flow to Orifice. *Colloids Surf.* **1991**, *56*, 13−23.

(16) Soos, M.; Ehrl, L.; Bäbler, M. U.; Morbidelli, M. Aggregate Breakup in a Contracting Nozzle. *Langmuir* **2010**, *26*, 10−18.

(17) Blaser, S. Flocs in Shear and Strain Flows. *J. Colloid Interface Sci.* **2000**, *225*, 273−284.

(18) Blaser, S. Break-up of Flocs in Contraction and Swirling Flows. *Colloids Surf., A* **2000**, *166*, 215−223.

(19) Blaser, S. Forces on the Surface of Small Ellipsoidal Particles Immersed in a Linear Flow Field. *Chem. Eng. Sci.* **2002**, *57*, 515−526.

(20) Harshe, Y. M.; Lattuada, M.; Soos, M. Experimental and Modeling Study of Breakage and Restructuring of Open and Dense Colloidal Aggregates. *Langmuir* **2011**, *27*, 5739−52.

(21) Selomulya, C.; Amal, R.; Bushell, G.; Waite, T. D. Evidence of Shear Rate Dependence on Restructuring and Breakup of Latex Aggregates. *J. Colloid Interface Sci.* **2001**, *236*, 67−77.

(22) Zaccone, A.; Soos, M.; Lattuada, M.; Wu, H.; Babler, M. U.; Morbidelli, M. Breakup of Dense Colloidal Aggregates under Hydrodynamic Stresses. *Phys. Rev. E* **2009**, *79*, No. 061401, DOI: 10.1103/PhysRevE.79.061401.

(23) Kobayashi, M.; Adachi, Y. Breakup and Structure of Flocs in a Turbulent Flow. *AIP Conf. Proc.* **1999**, *469*, 140−141.

(24) Higashitani, K.; Iimura, K. Two-Dimensional Simulation of the Breakup Process of Aggregates in Shear and Elongational Flows. *J. Colloid Interface Sci.* **1998**, *204*, 320−327.

(25) Higashitani, K.; Iimura, K.; Sanda, H. Simulation of Deformation and Breakup of Large Aggregates in Flows of Viscous Fluids. *Chem. Eng. Sci.* **2001**, *56*, 2927−2938.

(26) Eggersdorfer, M. L.; Kadau, D.; Herrmann, H. J.; Pratsinis, S. E. Fragmentation and Restructuring of Soft-Agglomerates under Shear. *J. Colloid Interface Sci.* **2010**, *342*, 261−268.

(27) Potanin, A. A. On the Computer-Simulation of the Deformation and Breakup of Colloidal Aggregates in Shear-Flow. *J. Colloid Interface Sci.* **1993**, *157*, 399−410.

(28) Saha, D.; Babler, M. U.; Holzner, M.; Soos, M.; Lüthi, B.; Liberzon, A.; Kinzelbach, W. Breakup of Finite-Size Colloidal Aggregates in Turbulent Flow Investigated by Three-Dimensional (3d) Particle Tracking Velocimetry. *Langmuir* **2016**, *32*, 55−65.

(29) Saha, D.; Lüthi, B.; Holzner, M.; Soos, M.; Liberzon, A.; Kinzelbach, W. *Experimental Analysis of Aggregate Breakage in Turbulent Flow by 3d-Ptv*. In AIChE Annual Meeting, Conference Proceedings, 2011.

(30) Saha, D.; Soos, M.; Lüthi, B.; Holzner, M.; Liberzon, A.; Babler, M. U.; Kinzelbach, W. Experimental Characterization of Breakage Rate of Colloidal Aggregates in Axisymmetric Extensional Flow. *Langmuir* **2014**, *30*, 14385−14395.

(31) Becker, V.; Schlauch, E.; Behr, M.; Briesen, H. Restructuring of Colloidal Aggregates in Shear Flows and Limitations of the Free-Draining Approximation. *J. Colloid Interface Sci.* **2009**, *339*, 362−372.

(32) Zeidan, M.; Xu, B. H.; Jia, X.; Williams, R. A. Simulation of Aggregate Deformation and Breakup in Simple Shear Flows Using a Combined Continuum and Discrete Model. *Chem. Eng. Res. Des.* **2007**, *85*, 1645−1654.

(33) Pantina, J. P.; Furst, E. M. Elasticity and Critical Bending Moment of Model Colloidal Aggregates. *Phys. Rev. Lett.* **2005**, *94*, No. 138301, DOI: 10.1103/PhysRevLett.94.138301.

(34) Binder, C.; Feichtinger, C.; Schmid, H. J.; Thurey, N.; Peukert, W.; Rude, U. Simulation of the Hydrodynamic Drag of Aggregated Particles. *J. Colloid Interface Sci.* **2006**, *301*, 155−167.

(35) Kroupa, M.; Vonka, M.; Kosek, J. Modeling the Mechanism of Coagulum Formation in Dispersions. *Langmuir* **2014**, *30*, 2693−2702.

(36) Kroupa, M.; Vonka, M.; Soos, M.; Kosek, J. Size and Structure of Clusters Formed by Shear Induced Coagulation: Modeling by Discrete Element Method. *Langmuir* **2015**, *31*, 7727−7737.

(37) Bossis, G.; Brady, J. F. Dynamic Simulation of Sheared Suspensions. 1. General-Method. *J. Chem. Phys.* **1984**, *80*, 5141−5154.

(38) Bossis, G.; Quentrec, B.; Brady, J. F. Dynamic Simulation of a Sheared Suspension. *Abstr. Pap., Jt. Conf. − Chem. Inst. Can. Am. Chem. Soc.* **1983**, *186*, 43.

(39) Brady, J. F.; Bossis, G. Stokesian Dynamics. *Annu. Rev. Fluid Mech.* **1988**, *20*, 111−157.

(40) Lieu, U. T.; Harada, S. Stability of Restructured Non-Fractal Aggregates in Simple Shear Flow. *Adv. Powder Technol.* **2015**, *26*, 705−710.

(41) Horii, K.; Yamada, R.; Harada, S. Strength Deterioration of Nonfractal Particle Aggregates in Simple Shear Flow. *Langmuir* **2015**, *31*, 7909−7918.

(42) Harada, S.; Tanaka, R.; Nogami, H.; Sawada, M. Dependence of Fragmentation Behavior of Colloidal Aggregates on Their Fractal Structure. *J. Colloid Interface Sci.* **2006**, *301*, 123−129.

(43) Ladd, A. J. C.; Gang, H.; Zhu, J. X.; Weitz, D. A. Time-Dependent Collective Diffusion of Colloidal Particles. *Phys. Rev. Lett.* **1995**, *74*, 318−321.

(44) Riese, D. O.; Wegdam, G. H.; Vos, W. L.; Sprik, R.; Fenistein, D.; Bongaerts, J. H. H.; Grubel, G. Effective Screening of

Hydrodynamic Interactions in Charged Colloidal Suspensions. *Phys. Rev. Lett.* **2000**, *85*, 5460−5463.
(45) Padding, J. T.; Louis, A. A. Hydrodynamic and Brownian Fluctuations in Sedimenting Suspensions. *Phys. Rev. Lett.* **2004**, *93*, No. 220601, DOI: 10.1103/PhysRevLett.93.220601.
(46) Banchio, A. J.; Gapinski, J.; Patkowski, A.; Haussler, W.; Fluerasu, A.; Sacanna, S.; Holmqvist, P.; Meier, G.; Lettinga, M. P.; Nagele, G. Many-Body Hydrodynamic Interactions in Charge-Stabilized Suspensions. *Phys. Rev. Lett.* **2006**, *96*, No. 138303, DOI: 10.1103/PhysRevLett.96.138303.
(47) Lin, N. Y. C.; Guy, B. M.; Hermes, M.; Ness, C.; Sun, J.; Poon, W. C. K.; Cohen, I. Hydrodynamic and Contact Contributions to Continuous Shear Thickening in Colloidal Suspensions. *Phys. Rev. Lett.* **2015**, *115*, No. 228304, DOI: 10.1103/PhysRevLett.115.228304.
(48) Royall, C. P.; Eggers, J.; Furukawa, A.; Tanaka, H. Probing Colloidal Gels at Multiple Length Scales: The Role of Hydrodynamics. *Phys. Rev. Lett.* **2015**, *114*, No. 258302, DOI: 10.1103/PhysRevLett.114.258302.
(49) Harshe, Y. M.; Lattuada, M. Breakage Rate of Colloidal Aggregates in Shear Flow through Stokesian Dynamics. *Langmuir* **2012**, *28*, 283−292.
(50) Ren, Z.; Harshe, Y. M.; Lattuada, M. Influence of the Potential Well on the Breakage Rate of Colloidal Aggregates in Simple Shear and Uniaxial Extensional Flows. *Langmuir* **2015**, *31*, 5712−5721.
(51) Cundall, P. A.; Strack, O. D. L. Discrete Numerical-Model for Granular Assemblies. *Geotechnique* **1979**, *29*, 47−65.
(52) Durlofsky, L.; Brady, J. F.; Bossis, G. Dynamic Simulation of Hydrodynamically Interacting Particles. *J. Fluid Mech.* **1987**, *180*, 21−49.
(53) Jeffrey, D. J. The Calculation of the Low Reynolds-Number Resistance Functions for 2 Unequal Spheres. *Phys. Fluids A* **1992**, *4*, 16−29.
(54) Jeffrey, D. J.; Onishi, Y. Calculation of the Resistance and Mobility Functions for 2 Unequal Rigid Spheres in Low-Reynolds-Number Flow. *J. Fluid Mech.* **1984**, *139*, 261−290.
(55) Liang, Y.; Hilal, N.; Langston, P.; Starov, V. Interaction Forces between Colloidal Particles in Liquid: Theory and Experiment. *Adv. Colloid Interface Sci.* **2007**, *134*−*135*, 151−166.
(56) Verwey, E. J. W.; Overbeek, J. T. G. *Theory of the Stability of Lyophobic Colloids*; Dover Publications: Mineola, NY, 1999; p xi.
(57) Israelachvili, J. N. *Intermolecular and Surface Forces: With Applications to Colloidal and Biological Systems*; Academic Press: London, 1985; p xv.
(58) Harada, S.; Tanaka, R.; Nogami, H.; Sawada, M.; Asakura, K. Structural Change in Non-Fractal Particle Clusters under Fluid Stress. *Colloids Surf., A* **2007**, *302*, 396−402.
(59) Pantina, J. P.; Furst, E. M. Elasticity and Critical Bending Moment of Model Colloidal Aggregates. *Phys. Rev. Lett.* **2005**, *94*, No. 138301, DOI: 10.1103/PhysRevLett.94.138301.
(60) Pantina, J. P.; Furst, E. M. Colloidal Aggregate Micromechanics in the Presence of Divalent Ions. *Langmuir* **2006**, *22*, 5282−5288.
(61) Pantina, J. P.; Furst, E. M. Micromechanics and Contact Forces of Colloidal Aggregates in the Presence of Surfactants. *Langmuir* **2008**, *24*, 1141−1146.
(62) Becker, V.; Briesen, H. Tangential-Force Model for Interactions between Bonded Colloidal Particles. *Phys. Rev. E* **2008**, *78*, 061404.
(63) Yu, N.; Polycarpou, A. A. Adhesive Contact Based on the Lennard-Jones Potential: A Correction to the Value of the Equilibrium Distance as Used in the Potential. *J. Colloid Interface Sci.* **2004**, *278*, 428−435.
(64) Tang, S.; Preece, J. M.; McFarlane, C. M.; Zhang, Z. Fractal Morphology and Breakage of Dlca and Rlca Aggregates. *J. Colloid Interface Sci.* **2000**, *221*, 114−123.
(65) Seto, R.; Botet, R.; Auernhammer, G. K.; Briesen, H. Restructuring of Colloidal Aggregates in Shear Flow: Coupling Interparticle Contact Models with Stokesian Dynamics. *Eur. Phys. J. E: Soft Matter Biol. Phys.* **2012**, *35*, 9805.